# THE ELECTRIC FIELD ALIGNMENT OF SHORT CARBON FIBRES TO ENHANCE THE TOUGHNESS OF EPOXY COMPOSITES

Anil R. Ravindran[1], Raj B. Ladani[1], Shuying Wu[1,2], Anthony J. Kinloch[3], Chun H. Wang[1,2] and Adrian P. Mouritz[1*]

[1]Sir Lawrence Wackett Aerospace Research Centre, School of Engineering, RMIT University, GPO Box 2476, Melbourne, VIC 3001, Australia.

[2]School of Mechanical and Manufacturing Engineering, University of New South Wales, Sydney, NSW 2052, Australia.

[3]Department of Mechanical Engineering, Imperial College London, South Kensington Campus, London SW7 2AZ, UK.

## ABSTRACT

An investigation is presented on increasing the fracture toughness of epoxy /short carbon fibre (SCF) composites by the alignment of short carbon fibres (SCFs) using an externally applied AC electric field. Firstly, the effects of the SCF length, SCF content and AC electric field strength on the rotational dynamics and alignment of the SCFs suspended in liquid (i.e. uncured) epoxy resin are quantified both experimentally and analytically. Secondly, it is shown that the mode I fracture toughness of the cured epoxy matrix composites increase rapidly with the weight fraction of SCFs up to a limiting value. The toughening effect is even greater when the SCFs are aligned in the composite normal to the direction of crack growth. Thirdly, it is found that alignment of the SCFs increases the fracture toughness by inducing multiple intrinsic and extrinsic toughening mechanisms, which are identified. Based on the identified the toughening mechanisms, an analytical model is proposed to predict successfully the enhancement of the fracture toughness due to the AC electric field alignment of the SCFs.

**Keywords:** A: Discontinuous reinforcement; B: Fracture toughness; C: Short carbon fibres; D: Epoxy polymer

**LIST OF SYMBOLS**

| | |
|---|---|
| $d_f$ | Diameter of a SCF |
| $l_{crit}$ | Critical length of the SCFs |
| $l_f$ | Length of a SCF |
| $l_{mea}$ | Measured pull-out length of the SCFs |
| $l_{po}$ | Pull-out length of the SCFs |
| $r_{yu}$ | Process zone radius ahead of the crack tip in the unmodified epoxy polymer |
| $t_r$ | Time to rotate a SCF from $\Theta_0$ *to* $\Theta'$ |
| $E_f$ | Young's modulus of the SCFs |
| $E_m$ | Young's modulus of the unmodified epoxy polymer |
| $E_o$ | Electric field strength |
| $G_{CU}$ | Quasi-static mode I fracture toughness of the unmodified epoxy |
| $G_i$ | Interfacial debonding energy between the SCFs and the epoxy matrix |
| $G_{Ic}$ | Quasi-static mode I fracture toughness of the epoxy/short carbon-fibre (SCF) composites |
| $K_{vm}$ | Maximum stress concentration for the von Mises stresses around a debonded SCF |
| $V_f$ | Volume fraction of SCFs |
| $V_{f\text{-}int}$ | Measured volume fraction of SCFs that were ruptured |
| $V_{po\text{-}\pm45°}$ | Calculated volume fraction of SCFs that are within an orientation distribution range from -45° to +45° |
| $V_{po\text{-}counted}$ | Measured volume fraction of SCFs that were pulled-out |
| $V_{void}$ | Volume fraction of voids in the epoxy polymer formed after debonding of the SCFs |
| $\varepsilon_m$ | Dielectric constant of the epoxy resin |
| $\varepsilon_{max}$ | Tensile failure strain of the SCFs |
| $\varepsilon_o$ | Vacuum permittivity |
| $\eta$ | Viscosity of the epoxy resin |
| $\nu$ | Poisson's ratio of the unmodified epoxy polymer |
| $\mu$ | Snubbing friction coefficient |
| $\mu_m$ | Pressure-dependent yield stress constant for the unmodified epoxy polymer |
| $\rho(\Theta)$ | Probability density of SCFs oriented within a given range |
| $\sigma_f$ | Tensile failure stress of the SCFs |
| $\sigma_y$ | Tensile yield stress of the unmodified epoxy polymer |
| $\tau_i$ | Interfacial shear failure stress of the SCF/epoxy, and/or interfacial shear friction stress under Tresca yield criterion |
| $\Delta G_{db}$ | Contribution to the overall increase in toughness from interfacial debonding between the SCFs and the epoxy polymer |
| $\Delta G_{pull\text{-}out}$ | Contribution to the overall increase in toughness from pull-out of the SCFs |
| $\Delta G_{rupture}$ | Contribution to the overall increase in toughness from rupture of the SCFs |
| $\Delta G_v$ | Contribution to the overall increase in toughness from plastic void growth of the epoxy polymer |
| $\Theta'$ | Relative angle between the SCF orientation and the applied electric field direction after $t_r > 0$s |
| $\Theta_0$ | Initial angle of a SCF suspended within the liquid epoxy resin relative to the applied electric field direction. |
| $\Theta_c$ | Critical angle of SCF relative to the crack propagation plane |
| $\Theta_f$ | SCF angle relative to the through-the-thickness direction |

## 1. INTRODUCTION

Thermosetting polymers, such as epoxy, are widely used in engineering structures as coatings, adhesives and polymer-matrix phase in fibre-reinforced composites. However, unmodified epoxies are relatively brittle materials and their fibre-reinforced composite materials have low interlaminar strength and fracture toughness [1]. The addition of a second phase, such as thermoplastic [2] or rubber [3, 4] particles, is a technique commonly used to increase the fracture toughness of epoxies. An alternative technique is with the addition of electrically conductive carbon based nanofillers to improve the fracture toughness of the epoxies. Significant increase in fracture properties can be achieved with relatively low concentrations, i.e. typically under about 2 wt.%. Proven nanofillers include carbon nanotubes (CNTs) [5], carbon nanofibres (CNFs) [1, 6] and graphene nanoplatelets (GnPs) [7]. Recent research has shown that carbon nanofillers, such as CNFs [1] and GnPs [7, 8], can be rapidly aligned in a liquid epoxy resin using an alternating current (AC) electric field [1, 7-9] or a direct current (DC) electric field [10]. It was found that the fracture toughness, $G_{Ic}$, increased significantly when the direction of crack growth was normal to the direction of alignment.

Another approach to improve the toughness of epoxies is the inclusion of short fibres at the sub-millimetre length and diameter scale, such as short carbon fibres (SCFs). It has been shown to enhance the fracture toughness, and other properties, of epoxies [6]. The appeal of using SCFs is their relatively low material and processing costs combined with their high stiffness and strength [11]. Studies have shown that SCFs extracted from waste material, such as off-cuts from dry carbon fabrics and pyrolized carbon fibre-polymer laminates, can be recycled and used as low-cost reinforcements, additives, interleaves and veils to improve the fracture toughness of bulk epoxy and fibre-reinforced epoxy composite materials [6, 11-14]. For example, Cholake et al. [11] demonstrated that blending 5.0 wt.% of milled and randomly oriented SCF into an epoxy yielded a 260% increase in the mode I fracture toughness, $G_{Ic}$. Due to the high dimensional aspect ratio of SCFs (i.e. being typically up to about 250), improvements to the properties of the resulting composite material are highly dependent on the orientation of the SCFs [15, 16]. Indeed, magnetophoretic techniques have been reported to align SCFs within liquid thermosetting and elastomeric resins [17, 18]. However, the electric field alignment of micron diameter scale SCFs in an epoxy resin, and its effect on the toughness of epoxy/SCF composites has not yet been reported.

The main aims of the present study are to investigate the toughness of epoxy/short carbon-fibre (SCF) composites and the effect of the alignment of the short carbon fibres (SCFs) using an externally applied AC electric field. Firstly, the dielectrophoresis mechanism controlling the rotation, orientation

and tethering of SCFs in the liquid (i.e. uncured) epoxy resin is investigated experimentally and analytically modelled. The procedure for aligning the SCFs in the epoxy resin can, therefore, be readily optimised with respect to the aspect ratio of the SCFs and the applied electric field strength. Secondly, the values of the mode I fracture toughness are determined for the (cured) epoxy/SCF composites containing different weight fractions of SCF, i.e. up to 10 wt.%. The SCFs were randomly orientated or aligned via the AC electric field procedure, as adapted from the previous author's work on CNF and GnPs [1, 7-9]. Thirdly, the toughening mechanisms responsible for the improvements in the fracture toughness due to the alignment of the SCFs are then identified. Finally, a model based on these toughening mechanisms is proposed and is used to successfully predict the experimentally measured values of the fracture toughness.

## 2. MATERIALS AND EXPERIMENTAL METHODOLOGY

### 2.1 SCF and Epoxy Materials

The SCFs, with an average diameter of 7 μm, were cut into 1.8 to 3.5 mm long sections from continuous carbon-fibre tows (T300 carbon fibres supplied by Colan Pty Ltd, Australia [19]) by using a paper guillotine, as shown in **Fig. 1**. The SCFs were then blended into the liquid epoxy resin at a weight fraction of 10 wt.% by hand-mixing for five minutes. The epoxy resin was a two-part blend of bisphenol-A and bisphenol-F resins (Resin 105® from West System, Australia). The SCF-epoxy mixture was then passed four times through a three-roll mill (Dermamill 100, Australia) operated at 50 rpm. The gap between the rotating rollers was progressively reduced with each pass of the epoxy-SCF mixture, down to a final gap size of 20 μm. This process separated the chopped SCF tows into individual fibres and dispersed them uniformly in the liquid epoxy resin. However, the shearing force generated in the three-roll milling process did fracture the SCFs and reduced their length, as may be seen from **Fig. 1(c)**. The average length of the SCFs after milling was 0.72 mm, with a standard deviation of ±0.21 mm, as shown in the length distribution plot in **Fig. 1(c)**. Following the milling process, the mixture which contained SCFs at a weight fraction of 10 wt.%, was diluted by adding more resin to obtain the other desired concentrations, i.e. 0.5, 1.0, 1.5, 2.0 and 5 wt.%. The epoxy hardener (Resin 206® from West System, Australia) used was a blend of aliphatic amines and aliphatic amine adducts based on diethylenetriamine and triethylenetetramine [20]. The hardener was added, at the concentration recommended by the supplier, to the epoxy resin mixture to activate cross-linking and curing, which was undertaken at room temperature, i.e. 25$^{o}$C for 48 h [20]. It should be noted that the given weight concentrations of the SCFs are relative to

the weight of the combined epoxy resin and hardener. The mixtures were hand-stirred and degassed to remove the entrapped air bubbles within the epoxy resin and hardener.

### 2.2 Electric field Alignment of SCFs

Two types of experiments were performed to study the alignment process. Either a single SCF or multiple SCFs were aligned in the liquid epoxy resin, without any hardener being present, using an externally applied AC electric field. **Fig. 2** presents a schematic of the apparatus used to measure the degree of alignment of the liquid epoxy resin containing a single or multiple SCFs when subjected to an applied AC electric field.

Firstly, for the single SCF studies, two parametric investigations were conducted to assess the influence of the length of the SCF and the strength of the AC electric field with respect to the time needed for rotation and alignment of the fillerin the liquid epoxy resin. The electric field was generated between two polymer-coated copper electrodes, with a 5.0 mm spacing, placed either side of the epoxy resin/single SCF mixture using an AC signal generator (Tektronix CFG250) along with a pre-amplifier (Kronhnkrit 7602M) operated at a frequency of 10 kHz. The single SCF was positioned approximately at an equal distance between the electrodes at an initial orientation of 88±0.5º relative to the direction of the applied electric field, which is taken to be the 0º direction. In assessing the effect of the length of the SCF, an electric field strength of 30V/mm was applied using a single SCF, that was 0.2, 0.6, 1.2 or 4.0 mm in length, in the liquid resin. Three values of the electric field strength, i.e. 30, 50 and 75 V/mm, were also investigated in the study of the influence of the AC electric field strength using an SCF, which was 0.6 mm in length, placed in the liquid epoxy resin.

Secondly, for evaluating the general effects of the electric field alignment of multiple SCFs in the liquid epoxy resin, the epoxy/SCFs mixture was poured on a glass slides between the two polymer-coated copper electrodes with a separation distance of 5.0 mm. The weight fraction of SCFs in the epoxy resin was 0.10 wt.%, and they were initially randomly orientated in the mixture. The electric field was generated (as described above) between the two electrodes using an AC signal generator along with a pre-amplifier, with a strength of 30 V/mm and operated at a frequency of 10 kHz.

In both studies, time-lapse photographic images were taken using a Leica optical microscope and videos were recorded using a Dynocapture USB microscope camera to observe the rotation and alignment of the single or multiple SCFs with increasing exposure time to the electric field. The orientation of the SCF(s) relative to the electric field direction was measured from the images using the ImageJ processing software.

### 2.3 Composite Manufacturing and Mode I Fracture Toughness Testing

The values of the mode I fracture toughness for the unmodified epoxy and the epoxy/SCF composites were measured using the double cantilever beam (DCB) test procedure described by Ladani et al. [7]. The DCB test specimens consisted of a 2 mm thick layer of the epoxy bonding two substrates, which were cured fibre reinforced polymer laminates and were 2.5 mm in thickness. These two composite substrates sandwiching the epoxy layer acted as the electrodes, as illustrated in **Fig. 3**. The substrate acting as the positive electrode was manufactured entirely from 12 plies of unidirectional T700 continuous carbon fibre/epoxy prepreg (VTM264, Lavender Composites, Australia). The negative electrode was made using a cured hybrid-fibre composite substrate consisting of ten plies of continuous unidirectional 'T700' carbon-fibre/epoxy-prepreg and two surface plies of continuous E-glass fibre/epoxy prepreg ('MTM57', Applied Composites Group, Australia). It should be noted that both composite arms of the DCB test had the same value of flexural modulus, within experimental error. The glass fibre plies in the negative electrode acted as a dielectric barrier to prevent short-circuiting during application of the AC electric field. The composites used for the positive and negative electrodes were cured and consolidated in an autoclave at 120°C and 620 kPa for one hour. The bonding surfaces of the substrates were then sand-blasted, cleaned in water, and finally degreased using acetone to remove any remaining surface impurities before being employed as the substrate materials.

The DCB specimens were manufactured by placing a mould made of mastic tape between the two composite substrates. The mould acted as a dam to prevent the liquid epoxy and hardener mixture from overflowing when poured between the substrates. The thickness of the epoxy layer was accurately controlled using 2 mm thick glass slides that were placed between the substrates and then removed after curing. For those specimens where alignment of the SCFs was to be studied, then an AC electric field with a strength of 30 V/mm and frequency of 10 kHz was applied between the composite electrodes to align the SCFs in the through-the-thickness direction, i.e. at $90^{o}$ to the electrodes. The AC electric field was applied during the first hour of the 48 h curing time at 25°C, since after about 1 h the viscosity of the epoxy and hardener mixture was relatively high and no further orientation of the SCFs could occur. The epoxy and hardener mixture was cured for 48 h at $25^{o}$C in accordance with resin supplier's guidelines [20].

Based on the manufacturing process, the DCB test specimens consisted of a 2 mm thick layer of an unmodified epoxy or an epoxy/SCF composite, bonding together the composite substrates, which had acted as the positive and negative electrodes when the SCFs needed to be aligned (see **Fig. 3**). One end of

the DCB specimen contained a 40 mm long, 11 μm thick film of Teflon (polytetrafluoroethylene) that was located within the unmodified epoxy or epoxy/SCF composite layer, and was placed approximately at an equal distance between the composite substrates. This film acted to initiate the crack under mode I (tensile opening) loading. Before fracture testing, the DCB specimens were wedged at the pre-cracked end to extend the initial crack length to 50±2.5 mm in order to create a sharp crack tip. DCB tests were then performed in accordance with ISO 25217 [21] by loading the cracked end of the specimens at a displacement rate of 1 mm/min using a 10 kN Instron tension testing machine (Instron, Australia). The crack was forced to grow along the DCB specimen by increasing the crack opening displacement; and the applied load, displacement and crack length values were measured. The crack length was measured with the aid of a travelling optical microscope in order to locate accurately the crack tip. Using these data, the 'corrected beam theory' approach [21] was used to calculate the mode I fracture toughness, $G_{Ic}$. Five DCB samples were tested for the unmodified epoxy polymer and for each of the epoxy composites containing the different weight fractions of SCFs up to 10 wt.%. The SCFs were either randomly orientated or aligned in the direction of the electric field, i.e. normal to the direction of crack growth along the length of the DCB specimen. In all the DCB tests the crack grew cohesively through the unmodified epoxy or the epoxy composite layer. The manufacturing process described above are adapted from the previous author's work on the electric field alignment of CNFs and GnPs in epoxy composites [1, 7-9].

## 3. RESULTS AND DISCUSSION

### 3.1 Electric field Alignment of the SCFs

*3.1.1 Effect of SCF aspect ratio and AC electric field strength on SCF orientation*

The influence of the length of the SCF on the alignment process was investigated using a single SCF suspended in the liquid epoxy resin and exposed to an AC electric field strength of 30 V/mm at 10 kHz for increasing times. The length of the SCF was varied between 0.2 to 4.0 mm and, as shown in **Fig. 4(a)**. In essence, all these lengths of single SCFs aligned to $\pm 2^{o}$ of the direction of the applied electric field within 300 s, from an initial angle of $88^{o} \pm 0.5^{o}$. When a rod (e.g. single SCF) is suspended in a dielectric liquid, e.g. a liquid epoxy resin, and then subjected to an AC electric field, then the rod becomes polarised due its variance shape anisotropy, dielectric properties and electrical conductivity being different to that of the liquid resin. As a result, a greater density of opposing charges will be induced at the ends of the rod, as indicated in **Fig. 2(a)**. The interaction of this dipole with the electric field gradient during the dielectrophoresis process generates a torque which leads to rotation and alignment of the SCFs in the

direction of the applied electric field [22, 23]. Furthermore, the total time of 300s needed to reach almost perfect alignment with the direction of the electric field was very similar for the different lengths of SCFs, where the values of the aspect ratio were about 30 to 575. Interestingly, Kim and Shkel [22] have also reported a minimal influence of the length, or the aspect ratio, of short glass fibres on the total rotation time required when subjected to a AC electric field strength of greater than 700 V/mm. However, the aspect ratio of the fillers ranging between 10 to 33 was only reported [22].

The rotation rate of the single SCFs was more sensitive to the strength of the AC electric field than the length of the SCF particularily when the length of the single fibre was 4 mm (i.e. an ~575 aspect ratio). The time to align the single SCFs in the direction of the electric field decreased rapidly with increasing electric field strength, i.e. from 30, 50 to 75 V/mm, as shown in **Fig. 4(b)**. Wu et al. [8] showed that increasing the electric field strength increases the torque acting on conductive particles suspended in a dielectric liquid, and that this is responsible for the more rapid alignment of the SCFs. By treating a single SCF as a thin oblate spheroid and by assuming that there is no interaction with neighbouring fibres, the time, $t_r$, required to rotate the SCF from an initial angle, $\Theta_0$, under an AC electric field of strength, $E_o$, can be calculated using [8]:

$$t_r = \left( \frac{\pi}{2} - \frac{d_f}{l_f} \right) \frac{8\eta}{\pi \varepsilon_m \varepsilon_0 E_0^2} \ln \frac{\tan \theta_0}{\tan \theta'} \qquad (1)$$

This is based on the assumption that the electric field induced torque is balanced against the viscous torque acting on the SCF. The viscosity, $\eta$, dielectric constant, $\varepsilon_m$, of the epoxy and vacuum permittivity, $\varepsilon_o$, are 0.55 Pa.s [20], 6.0 [22] and 8.85 x $10^{-12}$ F/m [22], respectively. The terms $l_f$ and $d_f$ are the length and diameter of the SCF, respectively. $\Theta$' denotes the relative angle between the SCF orientation and the applied electric field direction. As shown in **Fig. 4**, the calculated rotation times from 88º to 2º are in agreement with the experimentally measured times. However, the model does not accurately capture the rotational trend with the experimentally measured values for the 4 mm long (or higher aspect ratio) filler. This may suggest that additional interactions could take place such as inertial effects due to geometry and flow or rotational instability due to dielectrophoresis [22]. Unstable flow imparts additional vorticity around the fibres resulting in a mismatch between (a) the viscous drag moment acting on the fibre and (b) the torque generated on the ends on fibre due to the charging of the fibres during the application of the AC electric field [22]. However, it is important to note that the proposed model is relatively simplistic. The derivation of the analytical formulation presumes that both moments (i.e. drag and dielectrophoresis) acting on the fibre are equal [8].

### *3.1.2 In-situ alignment studies of SCFs in liquid epoxy resin*

*In-situ* alignment studies were also conducted by measuring the dielectrophoretic response of multiple SCFs in the liquid epoxy resin when subjected to an AC electric field strength of 30 V/mm at 10 kHz. The liquid epoxy resin, without added hardener, contained a weight fraction of SCFs of 0.10 wt.%. **Fig. 5(a)** and **Fig. 5(b)** show the random orientation of the SCFs at t = 0 s (i.e. the time at which the electric field was first applied) and the aligned orientation of the SCFs at t = 300 s after the application of the electric field, respectively. **Fig. 5(b)** shows that chain-formation of the SCFs has occurred between the electrodes, and this was due to the opposing charges present at the ends of the SCFs during the dielectrophoresis process [22]. **Fig. 5(c)** presents the population density for the orientation of the SCFs before and after application of the electric field for 300s. The application of the electric field has resulted in about 90% of the SCFs being oriented within ±30° of the direction of the electric field within 300 s from the start of it being applied.

### *3.1.3 Effect of SCF content on fibre orientation distribution in cured epoxy composites*

The weight fraction of the SCFs in the epoxy composites had a strong influence on the alignment process under the externally-applied AC electric field. In quantifying the degree of alignment, polished cross-sections of the cured epoxy/SCF composite samples containing different contents of SCFs up to 10 wt.% were examined using an optical microscope to measure the 2D distribution of the fibre angles. The effects of the electric field, at a strength of 30 V/mm at 10 kHz with an application time of 1 h during curing, and weight content of the SCFs on the measured fibre angle distribution are shown in **Fig. 6**. In this figure, the angles $0^o$ and $90^o$ are the directions parallel and normal to the electric field direction, repectively. The results for the orientation frequency of the SCFs are grouped into the one of three ranges of their orientation distribution as: (a) -30° to +30°, (b) -60° to -30° and +30° to +60° and (c) -90° to -60° and +60° to +90°.

In a perfectly randomly orientated condition, there would be an equal proportion of SCFs at all angles. However, this was not the case for the epoxy/SCF composites that were not subjected to the electric field. Instead the highest proportions of SCFs are within the range of -90° to -60° and +60° to +90°, and this proportion increases as the SCF content is increased. These observations may be attributed due to the wetting of the composite substrates by the 'liquid epoxy + hardener + SCFs' mixture, followed by the shear flow induced alignment of the SCFs when casting this resin mixture between the composite substrates [24]. With an increase in the SCF concentration, the greater packing and increased fibre-fibre

contact density increases the probability of the fibres orientating along the flow direction or, in the case observed, along with the in-plane direction of the DCB specimen [25]. This behaviour is a well-known phenomenon and has been previously reported [24] as the fibre content is increased.

For the epoxy/SCF composites subjected to the AC electric field during their preparation, the proportion of SCFs aligned relatively close to the direction of the electric field, i.e. -30° to +30°, is highly dependent on the content of the SCFs. At the lowest content studied, i.e. 0.5 wt.%, about 55% of the SCFs were oriented within -30° to +30° of the electric field direction. However, the percentage of SCFs so closely aligned with the direction of the electric field decreased rapidly with increasing weight content.

*3.1.4 Optimisation of the procedure for orientating the SCFs in the epoxy composites*

From the above experimental and theoretical studies on the single SCFs in the liquid epoxy, several key observations were made. Firstly, the effect of the length of the SCF has a minimal influence on the time needed to rotate the SCF from ±88º to within ±2° relative to the direction of the applied AC electric field. Secondly, the effect of AC electric field strength is inversely related to the time needed to rotate the SCFs to within ±2° relative to the direction of the electric field. Thirdly, it was observed that there was a significant alignment of the SCFs after the composite had being subjected to an electric field of a strength of 30V/mm after 300 s, see **Fig. 5(b).** Therefore, this level of electric field strength and exposure period were selected for manufacturing the DCB epoxy/SCF composites, especially since (a) an AC electric field strength of 30V/mm for 300 s was readily achievable using the present epoxy/hardener combination and (b) it has been used previously and therefore the present results may be readily compared with previous results [1].

## 3.2 Fracture Toughness of the Epoxy/SCF Composites

*3.2.1 Effect of SCF content and alignment*

The effects of the weight content of SCFs and of subjecting the composite to the AC electric field on the measured fracture toughness, $G_{Ic}$, of the epoxy composites are shown in **Fig. 7**. It should be noted that crack growth always occurred in an unstable, i.e. stick-slip, manner and the locus of crack growth was always cohesive in the unmodified epoxy or the epoxy/SCF composites, midway between the two substrates. From **Fig. 7** it may be seen that the fracture toughness increased with the SCF content up to ~5 wt.%, above which it essentially reached a plateau with a greater than 10-fold increase in the value of $G_{Ic}$, compared to the unmodified epoxy. The observation that the value of $G_{Ic}$ attains a plateau with an increasing volume content of randomly-oriented short fibres in a polymer matrix has also been reported

by Nikpur et al. [26]. Subjecting the SCFs to an AC electric field, so as to attempt to orientate the SCFs towards the through-the-thickness of the epoxy composite, i.e. normal to the direction of crack growth, increased their toughening effect by about 30%, but only when their content in the epoxy was up to about 2 wt.%. The approximate 30% improvement was validated using an 'unpaired t-test' employing the values of the mean and standard deviation between the measured $G_{Ic}$ values from the corresponding SCF epoxy samples, with a sample size of fifteen. The difference between the samples that were exposed to the AC electric field and were not exposed to the electric field were considered to be statistically significant with a two tailed P-value less than 0.001, i.e. 99.9% confidence level. These findings demonstrate that the electric field alignment of the SCFs in the epoxy/SCF composites is an effective technique to toughen such materials, but only at relatively low contents of SCFs. Upon increasing the SCF content to above 5.0 wt.%, then the application of the electric field did not provide any additional enhancement to the fracture toughness, and this observation is further discussed below.

*3.2.2 Comparison to literature values*

The improvements to the fracture toughness values of the present epoxy/SCF composites are compared to results from previous studies in **Table 1**. The values of $G_{Ic}$ are similar for the present composites to those reported by Zhou et al. [27], where similar fibre lengths and SCF contents were used. On the other hand, for a significantly shorter SCF length, Cholake et al. [11] reported a much lower $G_{Ic}$ value of 940 J/m$^2$ at 5.0 wt.% of SCFs compared to the composite studied here, where the value of $G_{Ic}$ was 1770 J/m$^2$. Although, at a content of SCFs of 10.0 wt.%, similar values are obtained in the present study and by Cholake et al. [11]. While any differences may be attributed to the relatively low SCF length used by Cholake et al. [11], other factors such as matrix type [28] will influence the fracture toughness. Finally, the present study mainly addresses the effect of the electric field alignment on the fracture toughness, as shown in **Fig.** 7 and in **Table 1**. However, the overall level of improvements in the values of $G_{Ic,}$ compared to the unmodified epoxy polymer, are shown to be significantly greater in the present study than the values reported by Cholake et al. [11], Zhou et al. [27] and Zhang et al. [6].

*3.2.3 Toughening mechanisms*

Scanning electron microscopy (SEM) examination of the crack initiation region (i.e. at the onset of crack growth) for the epoxy/SCF composites revealed a number of intrinsic and extrinsic toughening mechanisms operative. These toughening mechanisms are illustrated schematically in **Fig. 8**. This figure

also shows the main difference due to electric field alignment of the SCFs, where a greater density of fibre pull-out occurs.

Irrespective of the whether epoxy samples were exposed to an applied electric field, ahead of the main crack front, the intrinsic toughening mechanisms identified were epoxy void growth, interfacial debonding of SCFs from the epoxy matrix, and some very limited sites of microcracking. As shown in **Fig. 9(a)**, fractographic evidence of void and interfacial debonding sites surrounding the SCFs from the epoxy matrix within the process zone ahead of the crack front was present. The voids are an indication of the high-strain plastic flow of the epoxy within the process zone. The tri-axial stress field within the process zone is sufficiently high to cause debonding of the SCFs from the epoxy, resulting in the epoxy void growth mechanism. The progressive interfacial debonding at the epoxy/SCF interfaces, followed by the growth of the voids, promotes toughening via the dissipation of plastic energy [29]. The extent of the interfacial debonding and void growth sites increased with the SCF content, contributing to the increased fracture toughness. Some of the SCFs fractured within the debonding sites (**Fig. 9(a))**, and this occurs when their interfacial bond strength with the epoxy exceeds the fibre rupture stress. Even though the 'T300' carbon fibres used as the SCFs have a relatively high tensile failure stress, the roll milling process is expected to weaken the fibres via fibre/fibre contact (i.e. abrasion) due to the small gap opening of the three-roll mill used to process the composites. The finding that the milling process broke many of the SCFs, and thereby reduced the range of fibre lengths, see **Fig. 1(b)**, is clear evidence of fibre damage having occurred. Debonding of the SCFs, which also initiated at the fibre ends, lead to the limited formation of multiple microcrack sites (typically under about 15 μm long) within the process zone ahead of the main crack front, as shown in **Fig. 9(b)**. However, the density of these microcracks was observed to be relatively low compared to the number of SCFs within the same volume. Other studies have recently reported similar intrinsic toughening mechanisms for epoxy matrix composites reinforced with randomly orientated SCFs [29], GnPs [8] and CNFs [1].

The extrinsic toughening mechanisms are illustrated in **Fig. 10**. These extrinsic toughening mechanisms take place behind the main crack front and were identified as: (a) fibre pull-out from the epoxy matrix, (b) bridging of the fibres across the crack faces, (c) snubbing, and (d) rupture of the SCFs. Firstly, **Table 2** presents the measured volume fraction, $V_{po\text{-}counted}$, of SCFs that were pulled-out and were measured on the fracture surfaces of the composites from using scanning electron micrographs. A total of twenty micrographs, each with a surface area of 500 μm by 500 μm, were analysed for each epoxy/SCF composite. Previous studies have employed this technique for composites containing CNFs [1], CNTs [30, 31] and glass fibres [32]. The areal density of SCFs that were pulled-out was significantly higher

when the SCFs were oriented normal to the crack growth direction. This condition arose upon the application of the AC electric field and when a relatively low SCF content, i.e. up to 2 wt.%, was present. At the higher contents of 2.5, 5 and 10 wt.% of SCFs the volume fractions of SCFs that were pulled-out from the aligned SCF composites were similar in value to those of the randomly orientated SCF composites. As discussed previously, this occurred because the SCFs found it increasingly difficult to align normal to the crack growth direction at high contents due to the increased fibre-to-fibre content impeding the rotation and alignment process under the applied electric field, as shown in **Fig. 6**. Now, an interfacial friction sliding stress is also induced as the debonded SCFs are pulled-out, and this also increases the fracture toughness [29, 33]. For significant energy dissipation to result from the work-of-friction during pull-out, the SCFs must be aligned near-normal to the crack growth direction. Therefore, the pull-out toughening mechanism was more dominant in the composites containing a low content of SCFs that were exposed to the electric field, and hence aligned, as illustrated schematically in **Fig. 8(b)**. Secondly, since the SCFs were much longer than the crack opening displacement near the crack tip, it was possible for the SCFs to bridge the crack, shown in **Fig. 10(a)**. Therefore, the SCFs generated discrete traction loads at each bridging site which lowered the stress exerted on the crack tip, thereby increasing the fracture toughness. Bridging of the crack faces by the SCFs more readily occurred when the SCFs were aligned nearly normal to the direction of crack growth. Thirdly, concurrently during crack fibre bridging, the energy due to pull-out of the SCFs is further enhanced by snubbing [32, 34, 35], as shown in **Fig. 10(b)**. Snubbing is a toughening mechanism whereby the bridged SCFs, which have a far higher modulus than the epoxy, are pressed laterally into the surrounding epoxy matrix as they attempt to rotate and align in the direction of the crack opening. In this process the SCFs cause local plastic deformation of the surrounding epoxy matrix thereby increasing the local interfacial shear friction stress. This increases the value of the fracture toughness. Snubbing is most effective as a toughening mechanism when the bridged SCFs are slightly misaligned from the crack-opening direction, since when perfectly aligned the SCFs simply pull-out. Because crack bridging is required for snubbing to occur, this mechanism accounts in part for the epoxy/SCF composites that were exposed to an electric field having higher toughness values compared to the randomly orientated SCF composites, at low contents of SCFs. Fibre pull-out will occur providing the SCFs were inclined below the critical angle, $\Theta_c$, relative to the fracture plane. Above the critical angle, fibres are more likely to fracture along the crack propagation plane. At higher contents, i.e. 2.5 to 10 wt.% of SCFs, where a higher proportion of fibres were aligned along 60º to 90º, further fractographic studies revealed that the SCFs were orientated nearly parallel along the crack propagation plane with no evidence of tensile rupture; suggesting that a lower proportion of those fibres would

participate in the toughening process due to fibre pull-out. **Table 2** also presents the measured volume fractions, $V_{f\text{-}int}$, of fibres that were ruptured, and these values were measured as described above.

*3.2.4 Modelling the Toughening Mechanisms*

In modelling the fracture energy contribution, the primary toughening mechanisms in the SCF composites that were considered included: (a) interfacial debonding of the SCFs, (b) plastic void growth of the epoxy matrix (enabled by the debonding mechanism), (c) pull-out of the SCFs and (d) rupture of the SCFs. These mechanisms can be analysed to compute their individual contributions to the fracture toughness, $G_{Ic}$, of the epoxy composites using:

$$G_{Ic} = G_{CU} + \Delta G_v + \Delta G_{db} + \Delta G_{rupture} + \Delta G_{pull-out} \quad (2)$$

where $G_{CU}$ is the toughness of the unmodified epoxy polymer and $\Delta G_v$, $\Delta G_{db}$, $\Delta G_{rupture}$ and $\Delta G_{pull\text{-}out}$ are the contributions to the overall toughness arising from the toughening mechanisms of plastic void growth in the epoxy matrix, debonding of the SCFs, rupture of the SCFs, and pull-out of the SCFs, respectively. The value of $G_{CU}$ for the epoxy used in this study was measured to be 136 J/m$^2$.

The fracture energy for debonding of a single SCF from the epoxy matrix can be calculated using [31]:

$$\Delta G_{db} = V_{po}\frac{l_{crit}G_i}{2d_f} = (V_{po-counted})\frac{l_{crit}G_i}{2d_f} \quad (3)$$

where $V_{po}$ is the volume fraction of SCFs pulled-out, $l_{crit}$ is the critical pull-out length and $d_f$ is the SCF diameter. Here we take $V_{po}$ to be equivalent to the measured volume fraction, $V_{po\text{-}counted}$, of SCFs that were pulled-out, as given in **Table 2**. The term $G_i$ is the interfacial debonding energy between the SCF and the epoxy matrix. For the present type of carbon fibres and an epoxy matrix, Liu et al. [36] measured the interfacial debonding energy to be 1600 J/m$^2$, and this value was used in the present study. Following interfacial debonding, plastic void growth of the epoxy polymer in the process zone ahead of crack further increases the fracture toughness. The energy contribution from the plastic void growth mechanism can be calculated from Huang and Kinloch [37]:

$$\Delta G_{Void} = \left(1+\frac{\mu_m}{\sqrt{3}}\right)^2 \left(V_{void} - V_f\right)\sigma_y r_{yu} K_{vm}^2 \quad (4)$$

where $K_{vm}$ is maximum stress concentration for the von Mises stresses around a debonded SCF and $\mu_m$ is a material constant allowing for the pressure-dependence of the yield stress of the unmodified epoxy [37]. The parameters $r_{yu}$ and $\sigma_y$ are the process zone radius at fracture and the tensile yield stress of the unmodified epoxy, respectively The radius of the process zone is calculated using [37]:

$$r_{yu} = \frac{1}{6\pi}\frac{E_m G_{cu}}{(1-\nu^2)\sigma_y^2} \quad (5)$$

where $E_m$ is tensile modulus and $\nu$ is Poisson's ratio of the unmodified epoxy polymer. From SEM fractographic observations, the volume fraction, $V_{void}$, of voids may be determined by assuming their shape to be a truncated cone where the diameter of the void is two times the diameter of the fibre. This results in $V_{void} = 1.5\ V_f$.

The SCFs either pull-out or fracture depending on their orientation and embedded length within the epoxy matrix. An SCF above a critical length will rupture because the pull-out stress exceeds the fibre fracture stress. Below the critical length, the SCFs will pull-out, and not rupture. The critical length, $l_{crit}$, for a single SCF which is aligned normal to the direction of crack growth can be calculated using the Kelly-Tyson formulation, i.e. $l_{crit} = \sigma_f d_f / 2\tau_i$ [29]. The longest length, $l_{po}$, of an SCF that can be pulled-out is then equal to half the critical length, i.e. $l_{po} \leq l_{crit}/2$, and is calculated using:

$$l_{po} = \frac{\sigma_f d_f}{4\tau_i} \quad (6)$$

where $\sigma_f$ is the tensile failure stress and $\tau_i$ is the interfacial shear failure stress of the SCF. Many different values of $\tau_I$, ranging from 21 MPa to 30 MPa, for an epoxy matrix/carbon fibre interface have been reported in [27] and [38], respectively. The maximum interfacial friction shear stress is defined by the tensile yield strength of the epoxy matrix, which using the Tresca yield criterion is $\tau_i$ = 25 MPa. The maximum $l_{crit}$ is calculated to be 505 µm, whereby the maximum possible pull-out length is $l_{po} = l_{crit}/2$ = 253 µm. Via fractographic analysis, the mean pull-out SCF length, $l_{mea}$, was measured to be approximately 116 µm; which is approximately equivalent to $l_{crit}/4$. This is the expected statistical average pull-out length, as reported in many studies for short fibre reinforced polymer composites [16, 29, 39].

When the length of the SCF exceeds the critical length, then the SCF ruptures and the contribution from $\Delta G_{rupture}$ is given by [40]:

$$\Delta G_{rupture} = \frac{V_{f-\mathrm{int}}\sigma_f l_{crit}\varepsilon_{\max}}{2} = \frac{V_{f-\mathrm{int}}\sigma_f^2 l_{crit}}{2E_f} \quad (7)$$

where $E_f$ is the Young's modulus and $\varepsilon_{max}$ is the tensile failure strain of a SCF, respectively, and $V_{f\text{-}int}$ is the measured volume fraction of SCFs that ruptured along the crack propagation plane, see **Table 2**.

The contribution to the overall toughness from pull-out of a single SCF which is perfectly aligned normal to the crack plane can be determined from the models of Hull [33] and Cottrell-Kelly [29, 41]:

$$\Delta G_{pull-out} = \frac{2V_{po}\tau_i l_{po}^2}{d_f} \quad (8)$$

where $V_{po}$ is the volume fraction of SCFs that are pulled-out from the fracture surface of the epoxy. However, most SCFs are pulled-out at an angle relative to the crack propagation plane. Fractographic examination revealed that the maximum fibre angle, $\Theta_{crit}$, was approximately 45°. So, considering snubbing effects on the pull-out energy for inclined fibres and the fibre orientation distribution for the corresponding epoxy composites, Eq. (6) can now be re-stated as [16, 32]:

$$\Delta G_{pull-out} = \int_{\theta_f=0°}^{\theta_f=\theta_{crit}} \left( \frac{2V_f \tau_i l_{po}^2}{d_f} \exp(\mu\theta_f) \right) \rho(\theta) \mathrm{d}\theta_f \quad (9)$$

where $\mu$, $\Theta_f$ *and* $\rho(\Theta)$ are respectively the snubbing friction coefficient, SCF angle and probability density of SCFs oriented within a given orientation, respectively. This model considers the density of SCFs within the orientation range from -45° to +45° taken from the fibre-orientation probability-density plot, based on a 2D orientation distribution presented in **Fig. 11.** The value of the density of the SCFs that were subjected to pull-out, as presented in **Table 2**, is confirmed by the calculated volume fraction, $V_{po\text{-}\pm45°}$, of fibres that have an orientation distribution ranging from -45° to +45°. $V_{po\text{-}\pm45°}$ was calculated by multiplying the corresponding volume fraction of the epoxy composites by the density of fibres that were within the orientation distribution range from -45° to +45° The $V_{po\text{-}\pm45°}$ values are within the bounds of the measured $V_{po\text{-}counted}$ values from the fractographic studies, which again suggests that any fibres above ~45° would fracture along the crack propagation plane.

Eq. (2) may now be used to calculate the fracture toughness, $G_{Ic}$, of the epoxy/SCF composites as a function of the content of the SCFs, whether they were randomly orientated or aligned. The values used in the calculations are given in **Tables 2** and **3.** A comparison of the experimentally measured values and predictions from the theoretical model for values of $G_{Ic}$ is presented for the epoxy/SCF composites in **Fig. 12**. For the epoxy/SCF composites which were subjected to the electric field, the agreement between the experimental and theoretical values is very good. For the randomly orientated SCF composites, the agreement is still good, although the theoretical predictions are somewhat low at intermediate contents of SCFs. However, considering that no fitting factors are involved in the theoretical calculations, and that all the various input parameters needed for the modelling studies were directly calculated or measured experimentally, the overall agreement between the experimentally measured values of $G_{Ic}$ and the predicted values is acceptable. The observed agreement provides clear confirmation that the proposed toughening mechanisms are indeed responsible for the observed increases in toughness of the epoxy/SCF composites.

**Fig. 13** presents a stack-bar plot of the calculated contributions to the improvement in the fracture energy from each of the toughening mechanisms. Clearly, the pull-out of the SCFs, which includes the snubbing mechanism, is the most dominant toughening mechanism followed by the role of interfacial debonding. The contribution from the toughening mechanism of plastic void growth in the epoxy matrix around debonded SCFs is relatively small.

## 4. CONCLUSIONS

Overall, it has been shown that the mode I fracture toughness, $G_{Ic}$, of epoxy polymers can be improved using short carbon fibres (SCFs) and that the values of $G_{Ic}$ can be further improved by aligning the SCFs using an external AC electric field, providing the SCF content is sufficiently low to minimise fibre/fibre contact which impeded the rotation and alignment process. The SCFs were aligned using an AC electric field generated between two parallel CFRP composite electrodes. This electric field was able to rotate and align the SCFs within the liquid (pre-cured) epoxy resin within a few minutes. The detailed conclusions are given below.

Firstly, experimental testing and modelling revealed that the rotation rate of the SCFs was inversely proportional to the electric field strength, but was only weakly dependent on the length of the SCFs. The effect of the content of the SCFs in the epoxy composite was such that the majority of the SCFs, i.e. about 85%, were oriented within ±30° of the direction of the electric field when their content was relatively low, i.e. up to 2 wt.%. At higher contents the SCFs were unable to align under the action of the electric field, due to the reduction of free space between the fibres which increased the probability of contact and prevented them from rotating within the liquid resin. These studies allowed the alignment process for the epoxy/SCF composites to be optimised.

Secondly, it was found that the fracture toughness, $G_{Ic}$, of the epoxy/SCF composites increased steadily with SCF content up to about 5 wt.%, above which it essentially reached a plateau with a greater than 10-fold increase in the value of $G_{Ic}$, compared to the unmodified epoxy. Subjecting the SCFs to the AC electric field, so as to orientate the SCFs in a direction through-the-thickness of the epoxy composite (i.e. normal to the direction of crack growth) increased their toughening effect by about 30%, but only when their content in the epoxy was up to about 2 wt.%. This observation was as expected from the alignment studies noted above.

Thirdly, the intrinsic toughening mechanisms induced by the SCFs which occur ahead of the crack tip were identified as being due to: (a) interfacial debonding of the SCFs from the epoxy matrix, (b) plastic void growth in the epoxy matrix around the debonded SCFs and (c) some very limited

microcracking. The extrinsic toughening mechanisms induced by the SCFs, which take place behind the main crack front, were identified as: (a) fibre pull-out from the epoxy matrix, (b) bridging of the fibres across the crack faces, (c) snubbing and (d) rupture of the SCFs.

Fourthly, a theoretical model based upon these toughening mechanisms was proposed to calculate the value of the toughness, $G_{Ic}$, of the epoxy/SCF composites. The experimental and analytically measured fracture toughness values were in good agreement. Further, the results from the analytical modelling quantitatively identified the contributions from the various toughening mechanisms.

Finally, the use an AC electric field may prove to be very useful in orientating micron-diameter sized SCFs in epoxy, and other thermosetting, polymers for industrial moulding, extrusion and lamination applications. Further research will be conducted to assess the effect of an electrical field to align short carbon fibres with respect to improving other functional properties, such as the electrical conductivity of such polymer-composite materials.

**Acknowledgements**

The authors kindly acknowledge the technical assistance of the RMIT Materials Testing Laboratory team and the RMIT Microscopy and Microanalysis Facility (RMMF) team. The authors are thankful for the financial support received from the Australian Research Council's Discovery Grant Program (DP140100778).

**REFERENCES**

[1] Ladani RB, Wu S, Kinloch AJ, Ghorbani K, Zhang J, Mouritz AP, et al. Improving the toughness and electrical conductivity of epoxy nanocomposites by using aligned carbon nanofibres. Compos Sci Technol. 2015;117:146-58.
[2] Hodgkin JH, Simon GP, Varley RJ. Thermoplastic toughening of epoxy resins: A critical review. Polym Adv Technol. 1998;9(1):3-10.
[3] Kinloch AJ, Shaw SJ, Tod DA, Hunston DL. Deformation and fracture behaviour of a rubber-toughened epoxy: 1. Microstructure and fracture studies. Polymer. 1983;24(10):1341-54.
[4] Sprenger S. Epoxy resins modified with elastomers and surface-modified silica nanoparticles. Polymer. 2013;54(18):4790-7.
[5] Ma C, Liu H-Y, Du X, Mach L, Xu F, Mai Y-W. Fracture resistance, thermal and electrical properties of epoxy composites containing aligned carbon nanotubes by low magnetic field. Compos Sci Technol. 2015;114:126-35.
[6] Zhang G, Karger-Kocsis J, Zou J. Synergetic effect of carbon nanofibers and short carbon fibers on the mechanical and fracture properties of epoxy resin. Carbon. 2010;48(15):4289-300.
[7] Ladani RB, Wu S, Kinloch AJ, Ghorbani K, Zhang J, Mouritz AP, et al. Multifunctional properties of epoxy nanocomposites reinforced by aligned nanoscale carbon. Materials & Design. 2016;94:554-64.
[8] Wu S, Ladani RB, Zhang J, Bafekrpour E, Ghorbani K, Mouritz AP, et al. Aligning multilayer graphene flakes with an external electric field to improve multifunctional properties of epoxy nanocomposites. Carbon. 2015;94:607-18.
[9] Ladani RB, Wu S, Kinloch AJ, Ghorbani K, Mouritz AP, Wang CH. Enhancing fatigue resistance and damage characterisation in adhesively-bonded composite joints by carbon nanofibres. Compos Sci Technol. 2017;149:116-26.
[10] Monti M, Natali M, Torre L, Kenny JM. The alignment of single walled carbon nanotubes in an epoxy resin by applying a DC electric field. Carbon. 2012;50(7):2453-64.

[11] Cholake ST, Moran G, Joe B, Bai Y, Singh Raman RK, Zhao XL, et al. Improved Mode I fracture resistance of CFRP composites by reinforcing epoxy matrix with recycled short milled carbon fibre. Construction and Building Materials. 2016;111:399-407.
[12] Zhang Z, Tan Y, Wang X, Lin Y, Wang L. Synergetic effects on the mechanical and fracture properties of epoxy composites with multiscale reinforcements: Carbon nanotubes and short carbon fibers. J Appl Polym Sci. 2016;133(22).
[13] Yu H, Longana ML, Jalalvand M, Wisnom MR, Potter KD. Pseudo-ductility in intermingled carbon/glass hybrid composites with highly aligned discontinuous fibres. Composites Part A: Applied Science and Manufacturing. 2015;73:35-44.
[14] Pimenta S, Pinho ST. Recycling carbon fibre reinforced polymers for structural applications: Technology review and market outlook. Waste Management. 2011;31(2):378-92.
[15] Jain LK, Wetherhold RC. Effect of fiber orientation on the fracture toughness of brittle matrix composites. Acta Metallurgica Et Materialia. 1992;40(6):1135-43.
[16] Fu SY, Lauke B. The fibre pull-out energy of misaligned short fibre composites. Journal of Materials Science. 1997;32(8):1985-93.
[17] Ciambella J, Stanier DC, Rahatekar SS. Magnetic alignment of short carbon fibres in curing composites. Compos Part B: Eng. 2017;109:129-37.
[18] Stanier DC, Ciambella J, Rahatekar SS. Fabrication and characterisation of short fibre reinforced elastomer composites for bending and twisting magnetic actuation. Composites Part A: Applied Science and Manufacturing. 2016;91, Part 1:168-76.
[19] TORAYCA. T300 Data Sheet CFA-001, (2017), http://www.toraycfa.com/pdfs/T300DataSheet.pdf (accessed 08.01.17)
[20] WestSystem, West System Epoxy/105resin Data, (2015), http://www.westsystem.com.au/files/products.resin_and_hardeners/west_system_r105_eng_data.pdf (accessed 10.02.17)
[21] ISO 25217 Adhesives -- Determination of the mode 1 adhesive fracture energy of structural adhesive joints using double cantilever beam and tapered double cantilever beam specimens. 2009.
[22] Kim GH, Shkel YM. Polymeric composites tailored by electric field. J Mater Res. 2004;19(4):1164-74.
[23] Prasse T, Cavaillé J-Y, Bauhofer W. Electric anisotropy of carbon nanofibre/epoxy resin composites due to electric field induced alignment. Compos Sci Technol. 2003;63(13):1835-41.
[24] Such M, Ward C, Potter K. Aligned Discontinuous Fibre Composites: A Short History. Journal of Multifunctional Composites. 2014;2(3):155-68..
[25] Sebaibi N, Benzerzour M, Abriak NE. Influence of the distribution and orientation of fibres in a reinforced concrete with waste fibres and powders. Construction and Building Materials. 2014;65:254-63.
[26] Nikpur K, Chen YF, Kardos JL. Fracture toughness of unidirectional short-fiber reinforced epoxy composites. Compos Sci Technol. 1990;38(2):175-91.
[27] Zhou H, Du X, Liu H-Y, Zhou H, Zhang Y, Mai Y-W. Delamination toughening of carbon fiber/epoxy laminates by hierarchical carbon nanotube-short carbon fiber interleaves. Compos Sci Technol. 2017;140:46-53.
[28] Wu S, Guo Q, Kraska M, Stühn B, Mai YW. Toughening epoxy thermosets with block ionomers: The role of phase domain size. Macromolecules. 2013;46(20):8190-202.
[29] Kim J-K, Mai Y-w. High strength, high fracture toughness fibre composites with interface control—A review. Compos Sci Technol. 1991;41(4):333-78.
[30] Fu S-Y, Chen Z-K, Hong S, Han CC. The reduction of carbon nanotube (CNT) length during the manufacture of CNT/polymer composites and a method to simultaneously determine the resulting CNT and interfacial strengths. Carbon. 2009;47(14):3192-200.
[31] Hsieh TH, Kinloch AJ, Taylor AC, Kinloch IA. The effect of carbon nanotubes on the fracture toughness and fatigue performance of a thermosetting epoxy polymer. Journal of Materials Science. 2011;46(23):7525.
[32] Norman DA, Robertson RE. The effect of fiber orientation on the toughening of short fiber-reinforced polymers. J Appl Polym Sci. 2003;90(10):2740-51.
[33] Hull D, Clyne TW. An introduction to composite materials. 2nd ed. ed. Cambridge ; New York: Cambridge University Press; 1996.
[34] Li VC, Wang Y, Backer S. A micromechanical model of tension-softening and bridging toughening of short random fiber reinforced brittle matrix composites. J Mech Phys Solids. 1991;39(5):607-25.
[35] Cox BN, Sridhar N. A traction law for inclined fiber tows bridging mixed-mode cracks. Mech Adv Mater Struct. 2002;9(4):299-331.
[36] Liu HX, Gu YZ, Li M, Zhang DM, Li YX, Zhang ZG. Temperature effect on interfacial bonding property of single-carbon fiber/epoxy resin composite. Polym Compos. 2012;33(8):1368-75.
[37] Huang Y, Kinloch AJ. Modelling of the toughening mechanisms in rubber-modified epoxy polymers - Part II A quantitative description of the microstructure-fracture property relationships. Journal of Materials Science. 1992;27(10):2763-9.

[38] Gargano A, Pingkarawat K, Pickerd VL, Ibrahim ME, Mouritz AP. Effect of fibre-matrix interfacial strength on the explosive blast resistance of carbon fibre laminates. Compos Sci Technol. 2017;138:68-79.
[39] Fu S-Y, Mai Y-W, Lauke B, Yue C-Y. Synergistic effect on the fracture toughness of hybrid short glass fiber and short carbon fiber reinforced polypropylene composites. Materials Science and Engineering: A. 2002;323(1–2):326-35.
[40] Mirjalili V, Hubert P. Modelling of the carbon nanotube bridging effect on the toughening of polymers and experimental verification. Compos Sci Technol. 2010;70(10):1537-43.
[41] Hull D. An introduction to composite materials. Cambridge: Cambridge University Press; 1981.
[42] Kim JK, Baillie C, Mai YW. Interfacial debonding and fibre pull-out stresses - Part I Critical comparison of existing theories with experiments. Journal of Materials Science. 1992;27(12):3143-54.

**Table 1**. Comparison of $G_{Ic}$ values of the epoxy/SCF composites measured in the present study with reported values in the literature. (For values of $G_{Ic}$ the standard deviations are given in brackets.)

| **Source** | **Fillers (fibre length)** | **Content (wt.%)** | **$G_{Ic}$ (J/m$^2$)** | **Improvement (%)** |
|---|---|---|---|---|
| Present study | Unmodified Epoxy | - | 136 (± 20) | - |
| | SCF-Without E-Field (720 μm ±210 μm)* | 1.0 | 710 (± 63) | 425 % |
| | SCF-Without E-Field (720 μm ±210 μm)* | 2.5 | 1240 (± 42) | 790 % |
| | SCF-Without E-Field (720 μm ±210 μm)* | 5.0 | 1770 (± 144) | 1200 % |
| | SCF-Without E-Field (720 μm ±210 μm)* | 10.0 | 1960 (± 160) | 1340 % |
| | SCF-With E-Field (720 μm ±210 μm) | 1.0 | 990 (± 81) | 625 % |
| | SCF-With E-Field (720 μm ±210 μm) | 2.5 | 1360 (± 110) | 885 % |
| Zhou et al. [27] | Unmodified Epoxy | - | 275 (± 50) | - |
| | SCF (750 μm ±200 μm)* | 1.0 | 770 (± 52) | 180 % |
| | SCF (750 μm ±200 μm)* | 2.5 | 1360 (± 330) | 390 % |
| Cholake et al. [11] | Unmodified Epoxy | - | 260 (± 10) | - |
| | SCF (200 μm ±100 μm)* | 5.0 | 940 (± 20) | 260 % |
| | SCF (200 μm ±100 μm)* | 10.0 | 2060 (± 50) | 690 % |
| Zhang et al. [6] | Unmodified Epoxy | - | 120 | - |
| | SCF (55 μm ±21 μm)* | 7.2 | 230 | 90 % |
| | SCF (55 μm ±21 μm)* | 14.3 | 370 | 210 % |
| | SCF (55 μm ±21 μm)* | 21.5 | 425 | 255 % |

*The SCFs within the epoxy were not subjected to an externally-applied AC or DC electric field.

**Table 2.** Measured values of the volume fraction of SCFs which pulled-out, $V_{po\text{-}counted}$, and which ruptured, $V_{f\text{-}int}$, from scanning electron fractographs. The measured volume fractions, $V_{po\text{-}\pm45}$, of the SCFs in the composites with an orientation distribution range from -45º to +45º, relative to the through-the-thickness direction, are also given. (Standard deviations are given in brackets.)

| **SCFs (wt.%)** | $V_f$ **(%)** | $V_{po\text{-}counted}$ **(%)** | | $V_{po\text{-}\pm45°}$ **(%)** | | $V_{f\text{-}int}$ **(%)** | |
|---|---|---|---|---|---|---|---|
| | | **Without E-Field** | **With E-Field** | **Without E-Field** | **With E-Field** | **Without E-Field** | **With E-Field** |
| 1.0 | 0.58 | 0.15 (±0.03) | 0.31 (±0.05) | ~ 0.16 | ~ 0.34 | 0.39 (±0.07) | 0.51 (±0.07) |
| 1.5 | 0.87 | 0.22 (±0.03) | 0.39 (±0.08) | ~ 0.17 | ~ 0.42 | 0.49 (±0.17) | 0.72 (±0.11) |
| 2.0 | 1.16 | 0.26 (±0.05) | 0.40 (±0.04) | ~ 0.23 | ~ 0.45 | 0.68 (±0.12) | 0.91 (±0.06) |
| 2.5 | 1.45 | 0.34 (±0.09) | 0.39 (±0.07) | ~ 0.29 | ~ 0.48 | 0.82 (±0.07) | 0.99 (±0.10) |
| 5.0 | 2.93 | 0.48 (±0.08) | 0.49 (±0.08) | ~ 0.48 | ~ 0.51 | 1.50 (±0.09) | 1.30 (±0.14) |
| 10.0 | 6.00 | 0.49 (±0.05) | 0.48 (±0.05) | ~ 0.49 | ~ 0.49 | 2.00 (±0.15) | 2.00 (±0.16) |

**Table 3**. Values used in the analytical modelling studies.

| **Parameter** | **Symbol** | **Unit** | **Value** | **Source** |
|---|---|---|---|---|
| SCF diameter | $d_f$ | μm | 7 | This study |
| SCF average length after milling | $l_f$ | μm | 720 | This study |
| Tensile strength of SCF | $\sigma_f$ | MPa | 3530 | [19] |
| Young's modulus of SCF | $E_f$ | GPa | 230 | [19] |
| Density of SCF | $\rho_f$ | kg/m$^3$ | 1760 | [19] |
| Density of unmodified epoxy | $\rho_e$ | kg/m$^3$ | 1011 | [20] |
| Tensile yield strength of unmodified epoxy | $\sigma_y$ | MPa | 50.5 | [20] |
| Young's modulus of unmodified epoxy | $E_m$ | GPa | 3.18 | [20] |
| Maximum von Mises stress concentration | $K_{vm}$ | - | 2.11 | [31] |
| Epoxy/SCF interfacial fracture energy | $G_i$ | J/m$^2$ | 1600 | [36] |
| Pressure dependent yield stress constant | $\mu_m$ | - | 0.2 | [37] |
| Snubbing friction coefficient | $\mu$ | | 1.25 | [42] |

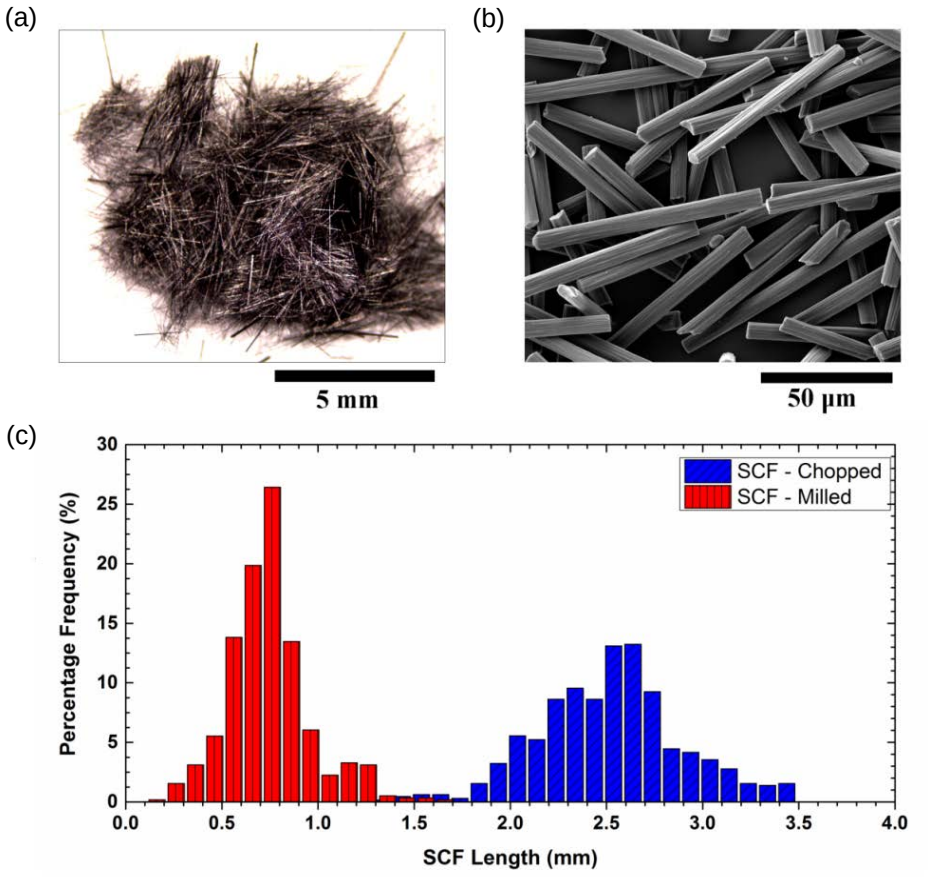


**Fig. 1.** Microscopy images of chopped SCFs (a) before (taken via optical microscopy) and (b) after the three-roll milling process (taken via scanning electron microscopy). (c) Frequency distribution plot of the lengths of the SCFs after and before the three-roll milling process.

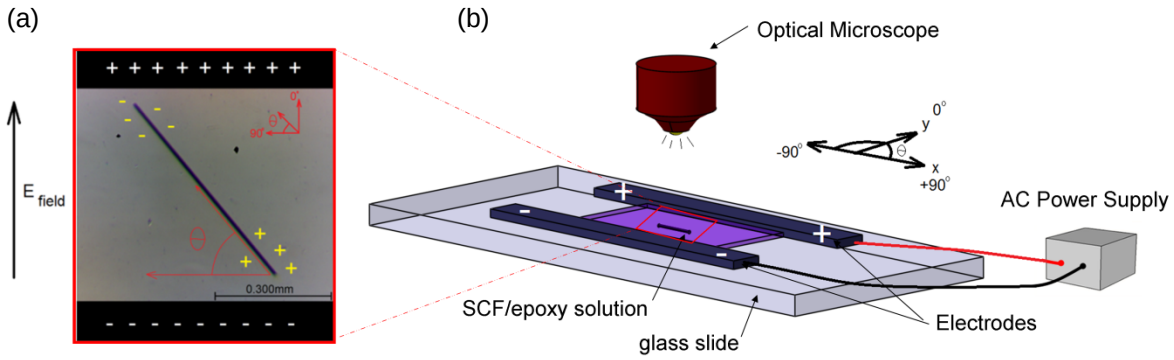


**Fig. 2.** (a) Schematic of a single SCF within the liquid epoxy resin during electric field alignment and (b) schematic of the test method used to electrically align and measure the angle of the single SCF.

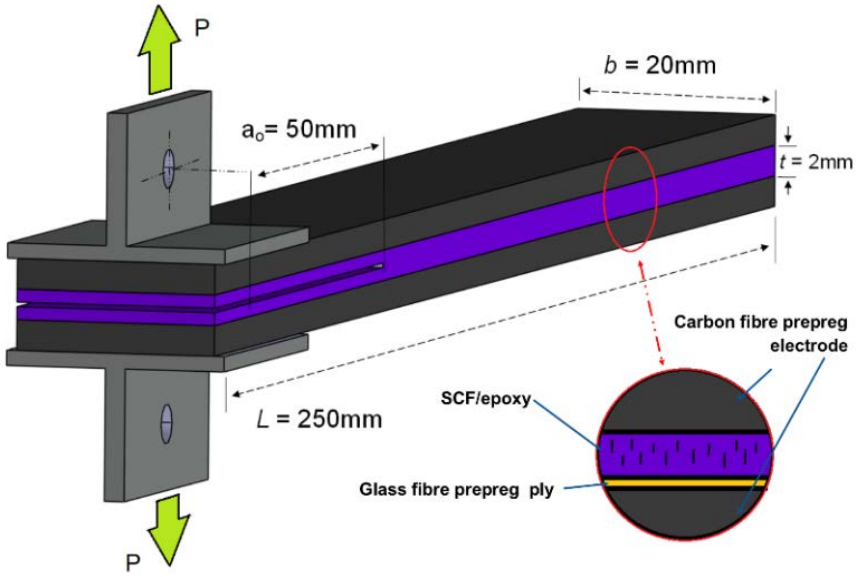


**Fig. 3.** Schematic and dimensions of the double cantilever beam (DCB) test specimen. The direction of the aligned SCFs is indicated.

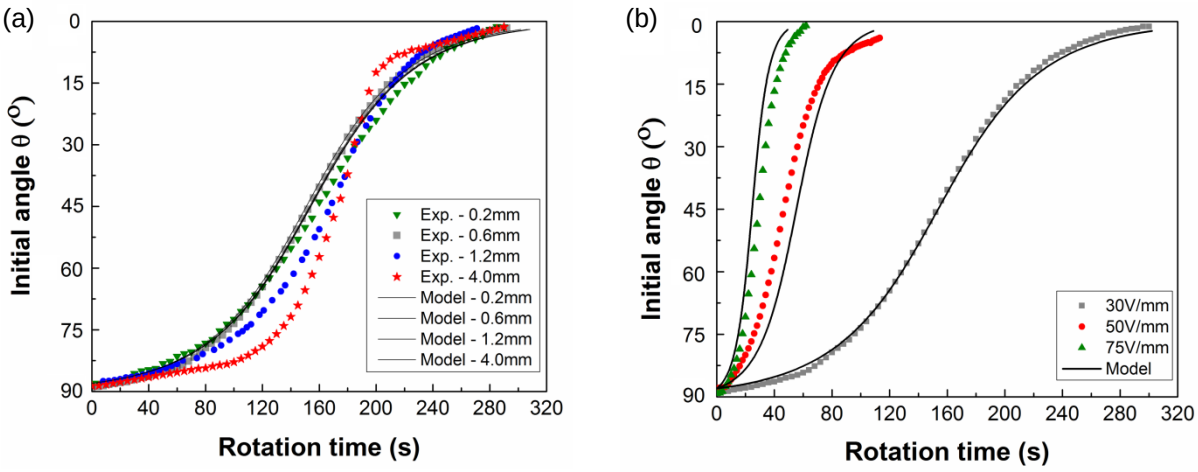


**Fig. 4.** Effects of (a) the fibre length (with an AC electric field strength of 30V/mm at 10 kHz) and (b) the AC electric field strength on the rotation time for a single SCF (0.6 mm length) in the liquid epoxy resin. (The rotation time is defined as the time needed to orient the fibres from the initial angle of ~88º to ~2º, i.e. 0º being the direction of the applied electric field.)

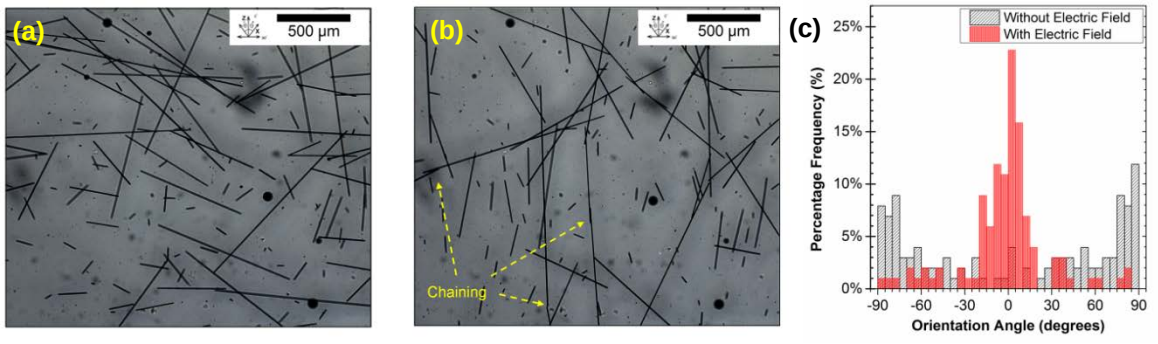


**Fig. 5**. *In-situ* alignment of 0.1 wt% SCFs in the liquid epoxy resin using an AC electric field strength of 30 V/mm at 10kHz. (a) t = 0 s containing randomly-oriented SCFs, (b) t = 300 s containing aligned SCFs and (c) comparison of the fibre-angle distribution of the SCFs before and after the AC electric field had been applied for 300 s.

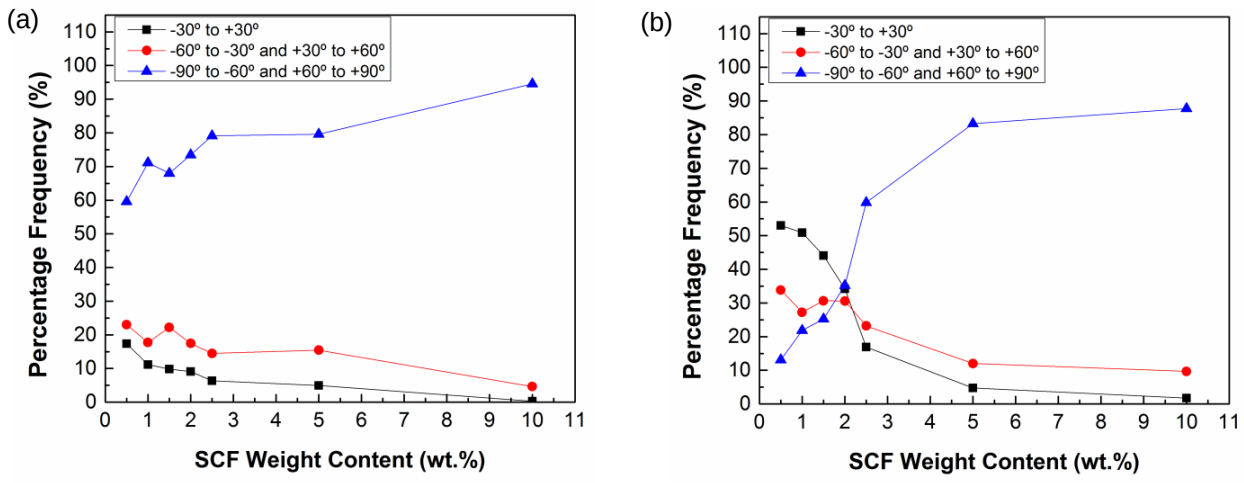


**Fig. 6**. Effect of SCF content on the distribution of the fibre angle of the epoxy/SCF composites (a) containing randomly orientated SCFs or (b) after the composites had been subjected to an AC electric field of 30V/mm at 10 kHz.

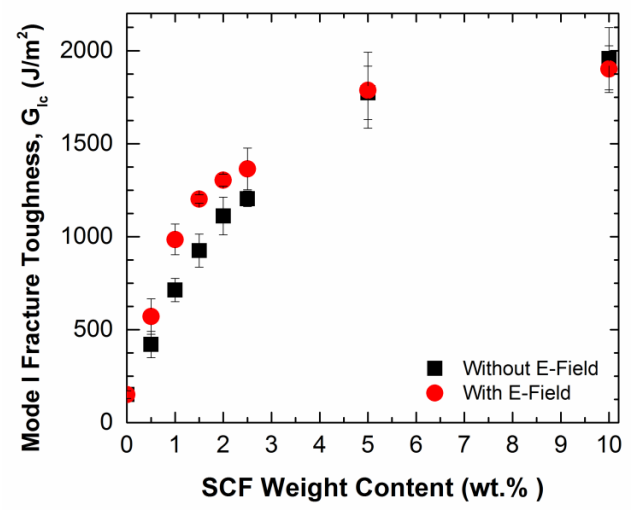


**Fig. 7**. Effect of SCF weight content on the mode I fracture toughness of the epoxy/SCF composites containing randomly orientated SCFs ('Without E-field) or after the composites had been subjected to an AC electric field of 30V/mm at 10 kHz ('With E-field').

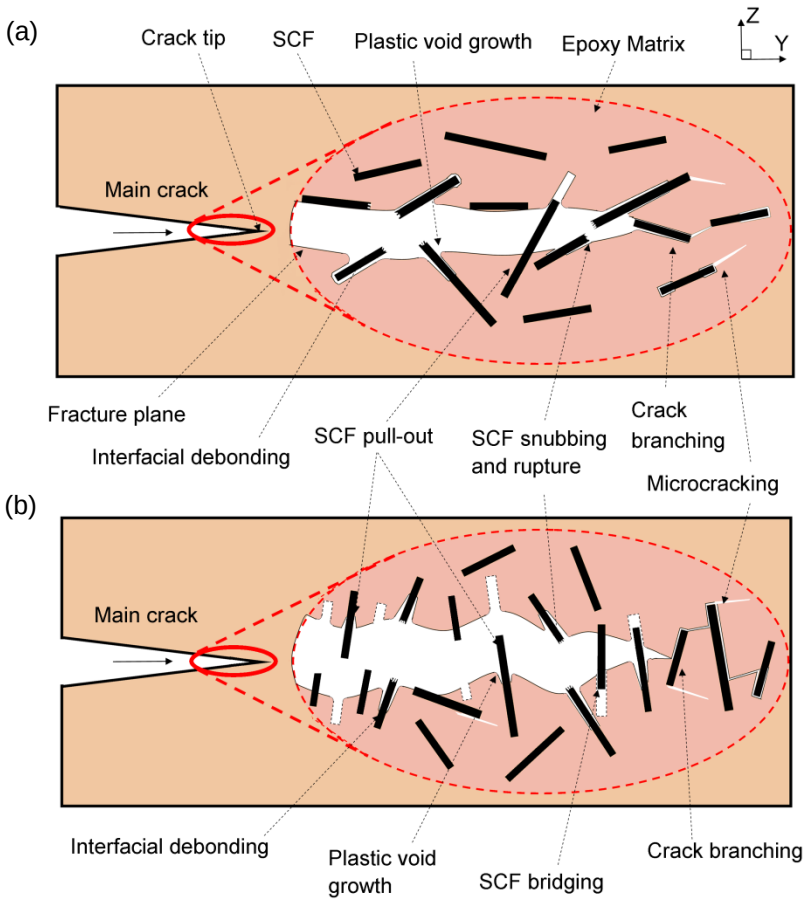


**Fig. 8**. Cross-sectional schematics of the toughening mechanisms operative during crack growth in the epoxy composites that contain (a) randomly aligned SCFs and (b) SCFs that were aligned by the externally applied AC electric field. (The inset of the area bound by the red dashed lines are a higher magnification schematic of the main crack tip encompassed by the solid red line.)

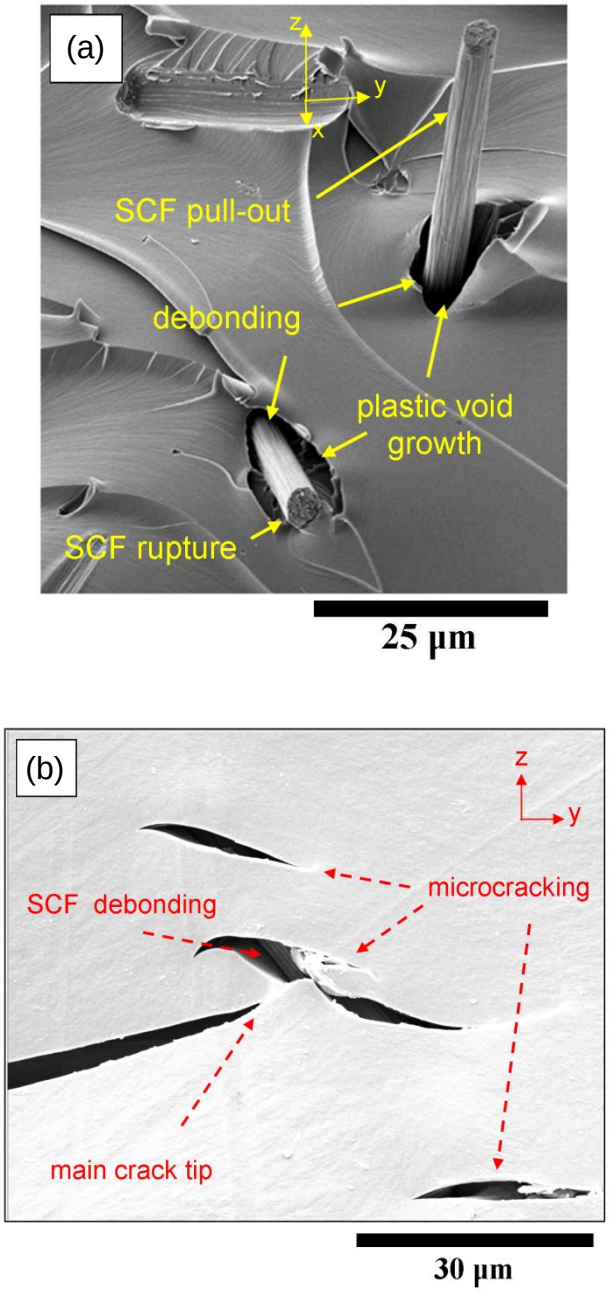


**Fig. 9**. Scanning electron micrographs of epoxy/SCF composites depicting the intrinsic toughening mechanisms within the process zone ahead of the main crack. (a) Of the fracture surface showing interfacial debonding and plastic void growth (for a 1.5 wt.% SCF composite subjected to an AC electric field of 30V/mm at 10 kHz) and (b) of the cross-section surrounding the main crack tip showing microcracking (for a 1.0 wt.% SCF composite subjected to an AC electric field of 30V/mm at 10 kHz).

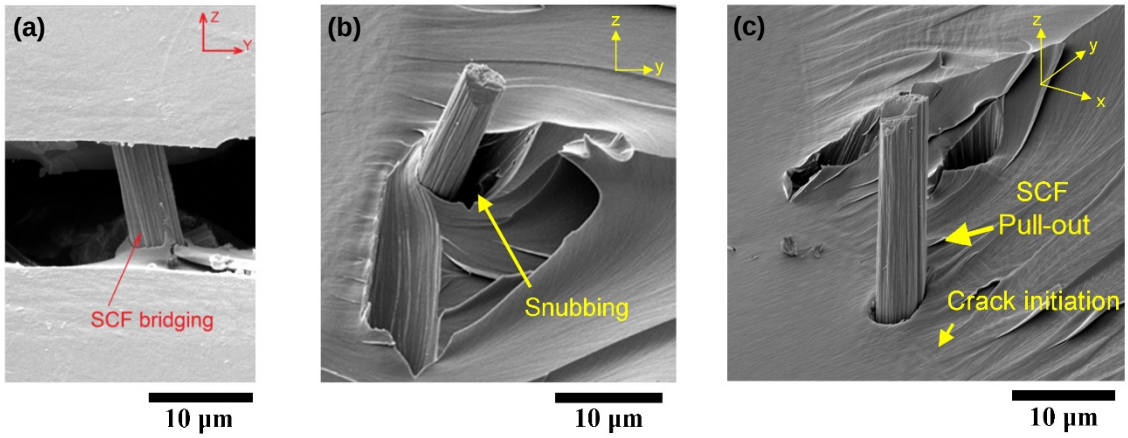


**Fig. 10**. Scanning electron micrographs showing examples of the extrinsic toughening mechanisms behind the main crack in the epoxy/SCF composites. (a) A SCF bridging the crack faces (for a 1.5 wt.% SCF composite subjected to an AC electric field of 30V/mm at 10 kHz), (b) SCF snubbing (for a 1.5 wt.% SCF composite subjected to an AC electric field of 30V/mm at 10 kHz) and (c) a SCF having been pulled-out (for a 1.0 wt.% SCF composite subjected to an AC electric field of 30V/mm at 10 kHz).

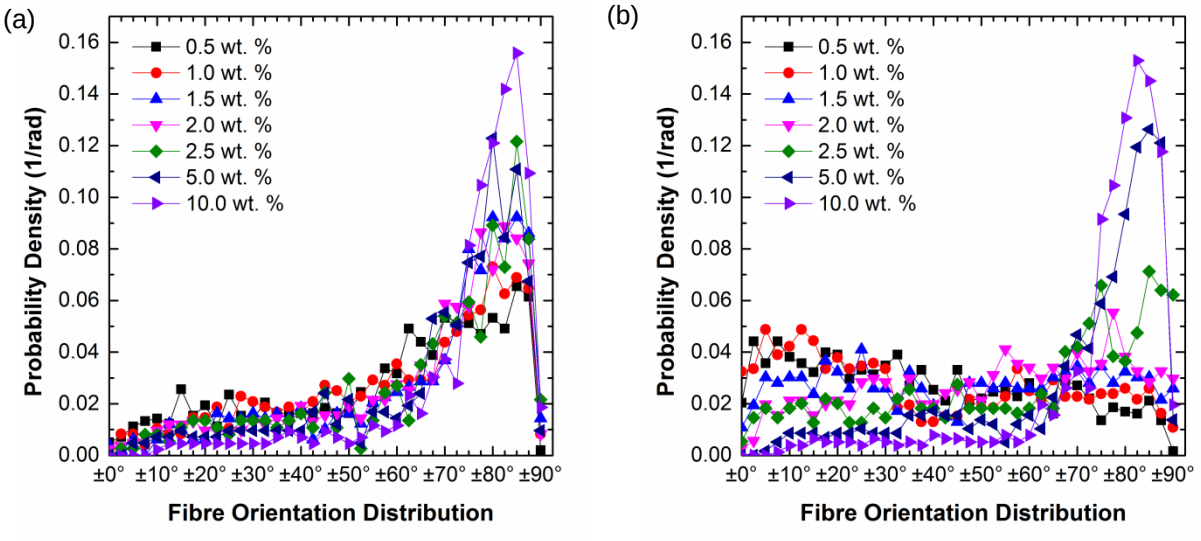


**Fig. 11**. 2D fibre orientation probability density of the SCFs in the epoxy/SCF composites (a) containing randomly orientated SCFs or (b) after the composites had been subjected to an AC electric field of 30V/mm at 10 kHz ('With E-field'). (Note: the probability density for each of the corresponding angles is in increments of ± 2.5º.)

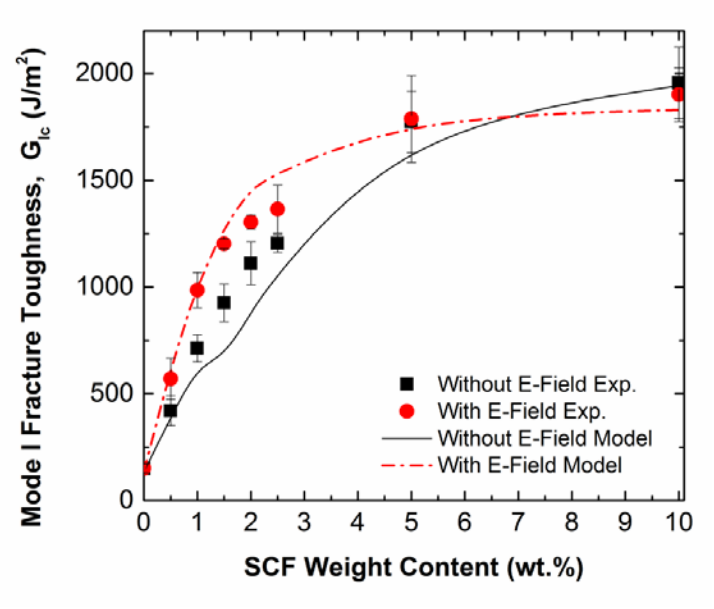


**Fig. 12.** Comparison of the experimental and analytically calculated values of the fracture toughness of the epoxy/SCF composites. The composites contained either randomly orientated SCFs (i.e. 'Without E-field') or where the composites had been subjected to an AC electric field of 30V/mm at 10 kHz (i.e. 'With E-field').

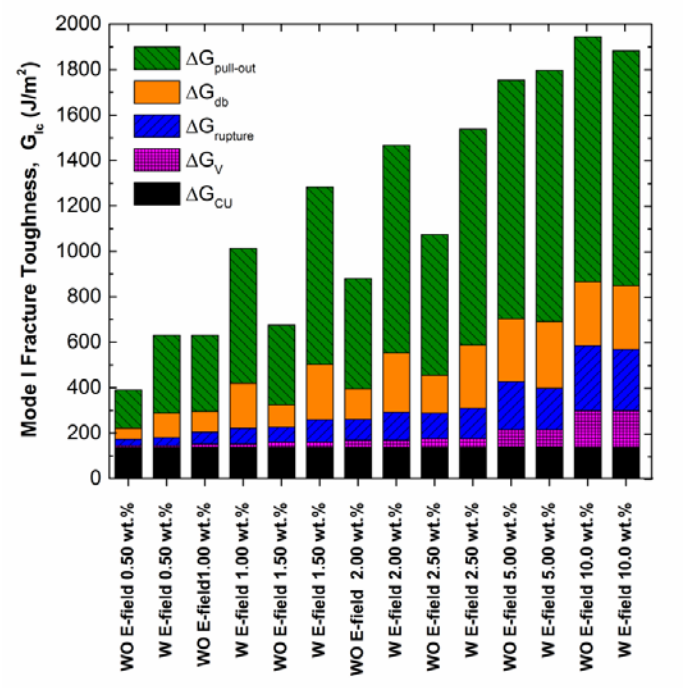


**Fig. 13.** Stack-bar plots of the contributions to the overall increase in toughness from the various toughening mechanisms from analytical calculations for the epoxy/SCF composites containing either randomly orientated SCFs (i.e. 'WO E-field') or where the composites had been subjected to an AC electric field of 30V/mm at 10 kHz (i.e. 'W E-field').